Advances in Nano Research, *Vol. 11, No. 4 (2021) 381-392*
https://doi.org/10.12989/anr.2021.11.4.381

Nonlinear electromechanical dynamics of piezoelectric doubly-curved microsystem using modified strain gradient theory

Dongxuan Wang*[1], Yazhou Xing[2] and Su Zhang[2]

[1]*College of science and technology, Hebei Agricultural University, Huanghua 061100, Hebei, China*
[2]*College of Mechanical and Electrical Engineering, Hebei Agricultural University, Baoding 071001, Hebei, China*

(*Received November 20, 2021, Revised August 5, 2021, Accepted August 11, 2021*)

Abstract. This paper is devoted to investigate the nonlinear free vibrations of multi-phase piezoelectric doubly-curved microshells in the context of modified strain gradient elastic (MSGT). The microshell has been made from two constituents for which different compositions have been considered by defining a piezoelectric phase percentage. The microscale effects have been described with the incorporation of three scale coefficients involved in MSGT. With the use of suitable Fourier series and the concept of Galerkin's method, the solution for the governing equations of double-curvature microshell have been provided. The calculated frequencies are dependent on the piezoelectric phase percentage, scale coefficients, curvature radius and applied electric voltage.
Keywords: doubly-curved shell; modified strain gradient theory; multi-phase material; nonlinear vibration; piezoelectric material

1. Introduction

An example for a smart material is piezoelectric-elastic material in which electric environments may lead to mechanical deformation (Aboudi 2001, Pan and Han 2005, Li and Pan 2015). This means that there is a coupling between electric and elastic performances in such materials (Li and Shi 2009, Guo *et al*. 2016). In such materials, the material properties can be characterized by elastic, piezoelectric and even magnetic constants. Structural components (beams, shells and plates) made of such smart materials are broadly utilized in actuators, sensors and intelligent systems. The material distribution in these structures may be homogenous or non-homogenous. When the material profile is variable thorough the thickness of a structure, the material distribution may be non-homogenous. As an example, a functional graded material is a non-homogenous material in which two materials are involved and all material properties change from one material to another. Based on the percentage and volume fraction of each material, the complete behavior of the structure can be defined. Another example is multi-phase piezoelectric material with homogenous nature in which the constituents are combined with each other to create a composite-type material. In multi-phase piezoelectric composites, the volume fraction of each constituent has a remarkable effect on effective properties of the composite material. There are several investigations on smart piezoelectric-magnetic-elastic structures having different material distribution (Kumaravel *et al*. 2007, Annigeri *et al*. 2007).

Up to now, different studies have been devoted to mechanical characterization of materials and structures (Zhang *et al*. 2018, Zenggang *et al*. 2019, Zhao *et al*. 2020, Lv *et al*. 2020a, b, Zhang *et al*. 2021a, b, c, Deng *et al*. 2020, 2021, Duan *et al*. 2021, Chen *et al*. 2021, Feng *et al*. 2021, Huang *et al*. 2021, Kordestani *et al*. 2021, Jiang *et al*. 2021, Lv and Liu 2021, Wang *et al*. 2021, Xu *et al*. 2021). According to recent experiments and atomistic simulations, it is reported that the mechanical character of small-size piezo-electric and piezo-magnetic structures are relied on small scale effects (Barati 2017, Al-Maliki *et al*. 2019, Kunbar *et al*. 2020). However, owning to the fact that classic continuum mechanical modelling is classified as a size free model, analyzing and investigating mechanical characteristics of small size structures based on the classic continuum theory yields inaccurate findings and accordingly wrongful designs (Ebrahimi and Barati 2017, Fenjan *et al*. 2020a, b). Howbeit, the atomistic modeling and molecular simulations are powerful tools for describing the size-dependent characteristics of small size structures, their application is not more economical because of the extra computational attempts. To prevail over such problems, a variety of size-dependent elasticity models including the nonlocal elasticity theory (Eringen 1972), strains gradient elasticity theory, refined couple stresses theory (Yang *et al*. 2002) and etc, are established for incorporating small size effects via standardizing some scale parameters and have been broadly exerted for the designing and study of the mechanical character of micro or nano structures (Thai and Vo 2012, Eltaher *et al*. 2012, Mirjavadi *et al*. 2020a, b, c, d, e, f, g, h, i, j, k, l, Abdulrazzaq *et al*. 2020, Ahmed *et al*. 2020a, b, Barati 2018a, b, c, Barati and Shahverdi 2018a, b, Ebrahimi and Barati a, b, c, d, e, f, g, h, Shariati *et al*. 2020a, b). The

*Corresponding author, Ph.D.,
E-mail: wangdongxuan278@126.com

ISSN: 2287-237X (Print), 2287-2388 (Online)

smart material discussed in previous paragraph has been extensively applied in micro/nano-structures and micro/nano-devices. However, at the microscale, the behavior of structure is dissimilar to macro scale counterparts. This is owning to the existence of small size effects. Such small size effects are incorporated in non-classical elasticity theories such as modified strain gradient theory (MSGT) which is also used by other authors. According to MSGT, three scale coefficients have been introduced which are shown to have the ability to describe microscale effects.

The present article has been devoted to investigate the nonlinear free vibrations of multi-phase piezoelectric doubly-curved microshells in the context of modified strain gradient elastic (MSGT). The microshell has been made from two constituents for which different compositions have been considered by defining a piezoelectric phase percentage. The microscale effects have been described with the incorporation of three scale coefficients involved in MSGT. With the use of suitable Fourier series and the concept of Galerkin's method, the solution for the governing equations of double-curvature microshell have been provided. The calculated frequencies are dependent on the piezoelectric phase percentage, scale coefficients, curvature radius and applied electric voltage.

2. Piezoelectric composites

A doubly-curved microshell of dimension L and b has been shown in Fig.1. This doubly curved microshell is made of a piezoelectric composite having two phases: a piezoelectric phase $BaTiO_3$ with volume fraction V_f and a piezo-magnetic phase $CoFe_2O_4$. All of material properties for the phases can be found in Table 1 which contains elastic (C_{ij}) and piezoelectric (e_{ij}) coefficients. Furthermore, k_{ij} expresses the dielectric constant (Mirjavadi *et al*. 2020a, b, c, d, e, f, g).

3. Basic equations according to MSGT

Utilizing Hamilton's rule in the subsequent manner, the governing equations may be established:

$$\int_0^t \delta(\Pi_S - \Pi_K + \Pi_W)dt = 0 \tag{1}$$

Here, Π_S, Π_K and Π_W exhibit the strain energy, kinetic energy and energy of exterior force. The strain energy for the model in hand may be achieved as a function of electrical field (E_x, E_y, E_z) and electrical field displacements (D_i):

$$\begin{aligned}\Pi_S = \int_V (&S_{xx}\delta\varepsilon_{xx} + S_{yy}\delta\varepsilon_{yy} + S_{xy}\delta\gamma_{xy}\\ &+\tau_{xxx}\delta\varsigma_{xxx} + \tau_{yxx}\delta\varsigma_{yxx} + \tau_{zxx}\delta\varsigma_{zxx} + \tau_{xyy}\delta\varsigma_{xyy}\\ &+\tau_{yyy}\delta\varsigma_{yyy} + \tau_{zyy}\delta\varsigma_{zyy} + \tau_{xxy}\delta\varsigma_{xxy}\\ &+\tau_{yxy}\delta\varsigma_{yxy} + \tau_{zxy}\delta\varsigma_{zxy} + \tau_{yxz}\delta\varsigma_{yxz}\\ &+\tau_{yyz}\delta\eta_{yyz} - D_x\delta E_x - D_y\delta E_y - D_z\delta E_z)dV\end{aligned} \tag{2}$$

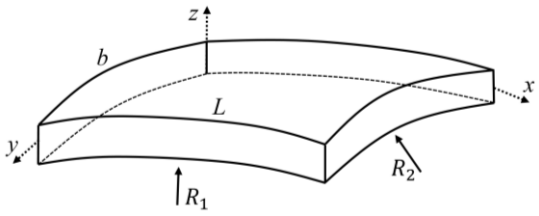

Fig. 1 A doubly-curved microshell

in such a way that S_{ij} and τ_{ijk} respectively exhibit the stress and double stress tensors; ε_{ij} and ς_{ijk} exhibit strain field and strain gradients. By taking into account the plane stress condition, all components of S_{ij}, D_i and τ_{ijk} should be expressed by:

$$S_{xx} = \tilde{C}_{11}\varepsilon_{xx} + \tilde{C}_{12}\varepsilon_{yy} - \tilde{e}_{31}E_z \tag{3}$$

$$S_{yy} = \tilde{C}_{12}\varepsilon_{xx} + \tilde{C}_{11}\varepsilon_{yy} - \tilde{e}_{31}E_z \tag{4}$$

$$S_{xy} = \tilde{C}_{66}\gamma_{xy} \tag{5}$$

$$D_x = +\tilde{k}_{11}E_x \tag{6}$$

$$D_y = +\tilde{k}_{11}E_y \tag{7}$$

$$D_z = \tilde{e}_{31}\varepsilon_{xx} + \tilde{e}_{31}\varepsilon_{yy} + \tilde{k}_{33}E_z \tag{8}$$

$$\tau_{xxx} = Y_1\varsigma_{xxx} + Y_2\varsigma_{xyy} + Y_3\varsigma_{yxy} \tag{9}$$

$$\tau_{yxx} = Y_2\varsigma_{yyy} + Y_5\varsigma_{yxx} + Y_4\varsigma_{xxy} \tag{10}$$

$$\tau_{zxx} = Y_5\varsigma_{zxx} + w_1\varsigma_{yyz} + 2w_2\varsigma_{zyy} \tag{11}$$

$$\tau_{xyy} = Y_4\varsigma_{yxy} + Y_2\varsigma_{xxx} + Y_5\varsigma_{xyy} \tag{12}$$

$$\tau_{yyy} = Y_2\varsigma_{yxx} + Y_3\varsigma_{xxy} + Y_1\varsigma_{yyy} \tag{13}$$

$$\tau_{zyy} = 2w_2\varsigma_{zxx} + Y_5\varsigma_{zyy} + Y_4\varsigma_{yyz} \tag{14}$$

$$\tau_{xxy} = \tau_{xyx} = 0.5Y_3\varsigma_{yyy} + Y_6\varsigma_{xxy} + 0.5Y_4\varsigma_{yxx} \tag{15}$$

$$\tau_{yxy} = \tau_{yyx} = 0.5Y_4\varsigma_{xyy} + 0.5Y_3\varsigma_{xxx} + Y_6\varsigma_{yxy} \tag{16}$$

$$\tau_{zxy} = \tau_{zyx} = 2w_4\varsigma_{zxy} + w_5\varsigma_{yxz} \tag{17}$$

in which Y_i are:

$$\begin{aligned}Y_1 &= 2(w_1 + w_2 + w_3 + w_4 + w_5)\\ Y_2 &= w_1 + 2w_2\\ Y_3 &= w_1 + 2w_3\\ Y_4 &= w_1 + 2w_5\\ Y_5 &= 2(w_2 + w_4)\\ Y_6 &= w_3 + 2w_4 + w_5\end{aligned} \tag{18}$$

In regard to the MSGT explained by Wang *et al*. (2013), the values of w_i should be taken as:

$$
\begin{aligned}
w_1 &= \mathrm{C}_{66}(l_2^2 - \frac{4}{15}l_1^2);\\
w_2 &= \mathrm{C}_{66}(l_0^2 - \frac{1}{15}l_1^2 - \frac{1}{2}l_2^2);\\
w_3 &= -\mathrm{C}_{66}(+\frac{4}{15}l_1^2 + \frac{1}{2}l_2^2);\\
w_4 &= \mathrm{C}_{66}(\frac{1}{3}l_1^2 + \mathrm{l}_2^2);\\
w_5 &= \mathrm{C}_{66}(\frac{2}{3}l_1^2 - \mathrm{l}_2^2);
\end{aligned}
\tag{19}
$$

Here, the scale coefficient l_0 exhibits the effect of dilatation gradient, l_1 and l_2 respectively exhibit the effects of deviatoric stretch gradient and symmetric rotation gradient. It must be explained that that by selecting $l_0=l_1=0$, the modified couple stress theory (MCST) may be rendered. Furthermore, supposing the plane stress conditions yields the below modified constants as:

$$
\begin{aligned}
&\tilde{C}_{11} = C_{11} - \frac{C_{13}^2}{C_{33}}, \tilde{C}_{12} = C_{12} - \frac{C_{13}^2}{C_{33}},\\
&\tilde{C}_{66} = C_{66}, \quad \tilde{e}_{31} = e_{31} - \frac{C_{13}e_{33}}{c_{33}},\\
&\tilde{k}_{11} = k_{11}, \quad \tilde{k}_{33} = k_{33} + \frac{e_{33}^2}{C_{33}}
\end{aligned}
\tag{20}
$$

The work because of the external loading can be determined by (Mirjavadi *et al*. 2020):

$$
\delta\Pi_W = \int_V (N_x^0 \frac{\partial(w)}{\partial x}\frac{\partial\delta(w)}{\partial x} + N_y^0 \frac{\partial(w)}{\partial y}\frac{\partial\delta(w)}{\partial y})dV \tag{21}
$$

in such as way that N_x^0, N_y^0 exhibit the exerted in-plane loading. The kinetic energy variation of the microshell should be determined by:

$$
\begin{aligned}
\delta\Pi_K = &\int_0^L\int_0^b [I_0(\frac{\partial u}{\partial t}\frac{\partial\delta u}{\partial t} + \frac{\partial v}{\partial t}\frac{\partial\delta v}{\partial t} + \frac{\partial w}{\partial t}\frac{\partial\delta w}{\partial t})\\
&-I_1(\frac{\partial u}{\partial t}\frac{\partial\delta w}{\partial x\partial t} + \frac{\partial w}{\partial x\partial t}\frac{\partial\delta u}{\partial t} + \frac{\partial v}{\partial t}\frac{\partial\delta w}{\partial y\partial t}\\
&+\frac{\partial w}{\partial y\partial t}\frac{\partial\delta v}{\partial t}) + I_2(\frac{\partial w}{\partial x\partial t}\frac{\partial\delta w}{\partial x\partial t} + \frac{\partial w}{\partial y\partial t}\frac{\partial\delta w}{\partial y\partial t})]dydx
\end{aligned}
\tag{22}
$$

where

$$
(I_0, I_1, I_2) = \int_{-0.5h}^{0.5h}(1, z, z^2)\rho dz \tag{23}
$$

4. Governing equations for doubly-curved microshells

By using thin shell theory for a doubly-curved microshell with curvatures (R_1, R_2), the three-dimensional displacement field which contains axial (u), circumferential (v) and transverse (w) components can be expressed as follows:

$$
u_1(x,y,z) = u(x,y) - z\frac{\partial w}{\partial x}(x,y) \tag{24}
$$

$$
u_2(x,y,z) = v(x,y) - z\frac{\partial w}{\partial y}(x,y) \tag{25}
$$

$$
u_3(x,y,z) = w(x,y) \tag{26}
$$

Above field components result in below relations foe the strain field:

$$
\begin{aligned}
\varepsilon_{xx} &= \frac{\partial u}{\partial x} + \frac{w}{R_1} - z\frac{\partial^2 w}{\partial x^2} + \frac{1}{2}\left(\frac{\partial w}{\partial x}\right)^2\\
\varepsilon_{yy} &= \frac{\partial v}{\partial y} + \frac{w}{R_2} - z\frac{\partial^2 w}{\partial y^2} + \frac{1}{2}\left(\frac{\partial w}{\partial y}\right)^2\\
\gamma_{xy} &= \frac{\partial u}{\partial y} + \frac{\partial v}{\partial x} - 2z\frac{\partial^2 w}{\partial x\partial y} + \frac{\partial w}{\partial x}\frac{\partial w}{\partial y}
\end{aligned}
\tag{27}
$$

According to the calculated strains, the strain gradients may be determined as:

$$
\begin{aligned}
&\varsigma_{xxx} = \frac{\partial^2 u}{\partial x^2} + \frac{1}{R_1}\frac{\partial w}{\partial x} - z\frac{\partial^3 w}{\partial x^3} + \frac{\partial w}{\partial x}\frac{\partial^2 w}{\partial x^2}\\
&= \varsigma_{xxx0} - z\varsigma_{xxx1}\\
&\varsigma_{yxx} = \frac{\partial^2 u}{\partial x\partial y} + \frac{1}{R_1}\frac{\partial w}{\partial y} - z\frac{\partial^3 w}{\partial x^2\partial y}\\
&+\frac{\partial^2 w}{\partial x\partial y}\frac{\partial w}{\partial x} = \varsigma_{yxx0} - z\varsigma_{yxx1}\\
&\varsigma_{zxx} = \varsigma_{zxx0} = -\frac{\partial^2 w}{\partial x^2}\\
&\varsigma_{xyy} = \frac{\partial^2 v}{\partial x\partial y} + \frac{1}{R_2}\frac{\partial w}{\partial x} - z\frac{\partial^3 w}{\partial x\partial y^2}\\
&+\frac{\partial^2 w}{\partial x\partial y}\frac{\partial w}{\partial y} = \varsigma_{xyy0} - z\varsigma_{xyy1}\\
&\varsigma_{yyy} = \frac{\partial^2 v}{\partial y^2} + \frac{1}{R_2}\frac{\partial w}{\partial y} - z\frac{\partial^3 w}{\partial y^3}\\
&+\frac{\partial w}{\partial y}\frac{\partial^2 w}{\partial y^2} = \varsigma_{yyy0} - z\varsigma_{yyy1}\\
&\varsigma_{zyy} = \varsigma_{zyy0} = -\frac{\partial^2 w}{\partial y^2}\\
&\varsigma_{xxy} = \varsigma_{xyx} = \frac{1}{2}(\frac{\partial^2 u}{\partial x\partial y} + \frac{\partial^2 v}{\partial x^2} - 2z\frac{\partial^3 w}{\partial x^2\partial y}\\
&+\frac{\partial^2 w}{\partial x^2}\frac{\partial w}{\partial y} + \frac{\partial w}{\partial x}\frac{\partial^2 w}{\partial x\partial y}) = \varsigma_{xxy0} - z\varsigma_{xxy1}\\
&\varsigma_{yxy} = \varsigma_{yyx} = \frac{1}{2}(\frac{\partial^2 u}{\partial y^2} + \frac{\partial^2 v}{\partial x\partial y} - 2z\frac{\partial^3 w}{\partial x\partial y^2}\\
&+\frac{\partial w}{\partial x}\frac{\partial^2 w}{\partial y^2} + \frac{\partial^2 w}{\partial x\partial y}\frac{\partial w}{\partial y}) = \varsigma_{yxy0} - z\varsigma_{yxy1}\\
&\varsigma_{zxy} = \varsigma_{zyx} = -\frac{\partial^2 w}{\partial x\partial y} = \varsigma_{zxy0}
\end{aligned}
\tag{28}
$$

The induced electric field having electric potential (Φ) to the doubly-curved micro-scale shell can be expressed as (Mirjavadi *et al*. 2020):

$$
\Phi(x,y,z) = -cos(\xi z)\phi(x,y) + \frac{2z}{h}V_E \tag{29}
$$

Next, V_E defines the exterior electrical voltages induced to the smart shell. All ingredients of electrical field (E_x, E_θ, E_z) can be obtained as:

$$E_x = -\Phi_{,x} = cos(\xi z)\frac{\partial \phi}{\partial x}, \tag{30}$$

$$E_y = -\Phi_{,y} = cos(\xi z)\frac{\partial \phi}{\partial y}, \tag{31}$$

$$E_z = -\Phi_{,z} = -\xi\, sin(\xi z)\phi - \frac{2V_E}{h} \tag{32}$$

With the help of Hamilton's rule and placing Eqs. (2), (21) and (22) into Eq. (1) yields four governing equations for the piezoelectric doubly-curved microshells:

$$\begin{aligned}&\frac{\partial N_{xx}}{\partial x}+\frac{\partial N_{xy}}{\partial y}-\frac{\partial^2 T_{xxx}}{\partial x^2}-\frac{\partial^2 T_{yxx}}{\partial x\partial y}-\frac{1}{2}\frac{\partial^2 T_{xxy}}{\partial x\partial y}\\&-\frac{1}{2}\frac{\partial^2 T_{yxy}}{\partial y^2}=I_0\frac{\partial^2 u}{\partial t^2}-I_1\frac{\partial^3 w}{\partial x\partial t^2}\end{aligned} \tag{33}$$

$$\begin{aligned}&\frac{\partial N_{xy}}{\partial x}+\frac{\partial N_{yy}}{\partial y}-\frac{\partial^2 T_{xyy}}{\partial x\partial y}-\frac{\partial^2 T_{yyy}}{\partial y^2}-\frac{1}{2}\frac{\partial^2 T_{xxy}}{\partial x^2}\\&-\frac{1}{2}\frac{\partial^2 T_{yxy}}{\partial x\partial y}=I_0\frac{\partial^2 v}{\partial t^2}-I_1\frac{\partial^3 w}{\partial y\partial t^2}\end{aligned} \tag{34}$$

$$\begin{aligned}&\frac{\partial^2 M_{xx}}{\partial x^2}+2\frac{\partial^2 M_{xy}}{\partial x\partial y}+\frac{\partial^2 M_{yy}}{\partial y^2}-\frac{N_{yy}}{R_2}\\&-\frac{N_{xx}}{R_1}+\frac{1}{R_1}\frac{\partial T_{xxx}}{\partial x}-\frac{\partial^3 M_{xxx}}{\partial x^3}+\frac{1}{R_1}\frac{\partial T_{yxx}}{\partial y}\\&-\frac{\partial^3 M_{yxx}}{\partial x^2\partial y}+\frac{\partial^2 T_{zxx}}{\partial x^2}+\frac{\partial^2 T_{zyy}}{\partial y^2}+\frac{1}{R_2}\frac{\partial T_{xyy}}{\partial x}\\&-\frac{\partial^3 M_{xyy}}{\partial x\partial y^2}+\frac{1}{R_2}\frac{\partial T_{yyy}}{\partial y}-\frac{\partial^3 M_{yyy}}{\partial y^3}\\&-\frac{\partial^3 M_{xxy}}{\partial x^2\partial y}-\frac{\partial^3 M_{yxy}}{\partial x\partial y^2}+\frac{\partial^2 T_{zxy}}{\partial x\partial y}\\&+(N_x^0+N_{xx})(\frac{\partial^2 w}{\partial x^2})+(N_y^0+N_{yy})(\frac{\partial^2 w}{\partial y^2})\\&+2N_{xy}\frac{\partial^2 w}{\partial x\partial y}=+I_0\frac{\partial^2 w}{\partial t^2}+I_1\frac{\partial^3 u}{\partial x\partial t^2}\\&+I_1\frac{\partial^3 v}{\partial y\partial t^2}-I_2(\frac{\partial^4 w}{\partial x^2\partial t^2}+\frac{\partial^4 w}{\partial y^2\partial t^2})\end{aligned} \tag{35}$$

$$\int_{-h/2}^{h/2}\begin{pmatrix}cos(\xi z)\dfrac{\partial D_x}{\partial x}+cos(\xi z)\dfrac{\partial D_y}{\partial y}\\+\xi\, sin(\xi z)D_z\end{pmatrix}dz=0 \tag{36}$$

Also, note that N_{ij}, T_{ij} and M_{ij} (ij = xx, xy, yy) describe membrane forces and bending moments:

$$\begin{aligned}(N_{xx},N_{yy},N_{xy})&=\int_{-0.5h}^{+0.5h}(S_{xx},S_{yy},S_{xy})dz\\(M_{xx},M_{yy},M_{xy})&=\int_{-0.5h}^{+0.5h}(S_{xx},S_{yy},S_{xy})zdz\\(T_{xxx},T_{yxx},T_{zxx})&=\int_{-0.5h}^{+0.5h}(\tau_{xxx},\tau_{yxx},\tau_{zxx})dz\\(T_{xyy},T_{yyy},T_{zyy})&=\int_{-0.5h}^{+0.5h}(\tau_{xyy},\tau_{yyy},\tau_{zyy})dz\\(T_{xxy},T_{yxy},T_{zxy})&=\int_{-0.5h}^{+0.5h}(\tau_{xxy},\tau_{yxy},\tau_{zxy})dz\\(M_{xxx},M_{yxx})&=\int_{-0.5h}^{+0.5h}(\tau_{xxx},\tau_{yxx})zdz\\(M_{xyy},M_{yyy})&=\int_{-0.5h}^{+0.5h}(\tau_{xyy},\tau_{yyy})zdz\\(M_{xxy},M_{yxy})&=\int_{-0.5h}^{+0.5h}(\tau_{xxy},\tau_{yxy})zdz\end{aligned} \tag{37}$$

Accordingly, N_x^0, N_y^0 define the in-plane loading owning to external electrical voltages V_E and is defined as:

$$N^E=-\int_{-h/2}^{h/2}\tilde{e}_{31}\frac{2V_E}{h}dz \tag{38}$$

Then, one can calculate the stress resultants through integration of Eq. (37) over the thickness of microshell as:

$$\begin{aligned}N_{xx}&=A_{11}(\frac{\partial u}{\partial x}-\frac{w}{R_1}+\frac{1}{2}(\frac{\partial w}{\partial x})^2)-B_{11}\frac{\partial^2 w}{\partial x^2}\\&+A_{12}(\frac{\partial v}{\partial y}-\frac{w}{R_2}+\frac{1}{2}(\frac{\partial w}{\partial y})^2)-B_{12}\frac{\partial^2 w}{\partial y^2}+A_{31}^e\phi\end{aligned} \tag{39}$$

$$\begin{aligned}M_{xx}&=B_{11}(\frac{\partial u}{\partial x}-\frac{w}{R_1}+\frac{1}{2}(\frac{\partial w}{\partial x})^2)-D_{11}\frac{\partial^2 w}{\partial x^2}\\&+B_{12}(\frac{\partial v}{\partial y}-\frac{w}{R_2}+\frac{1}{2}(\frac{\partial w}{\partial y})^2)-D_{12}\frac{\partial^2 w}{\partial y^2}+E_{31}^e\phi\end{aligned} \tag{40}$$

$$\begin{aligned}N_{yy}&=A_{12}(\frac{\partial u}{\partial x}-\frac{w}{R_1}+\frac{1}{2}(\frac{\partial w}{\partial x})^2)-B_{12}\frac{\partial^2 w}{\partial x^2}\\&+A_{11}(\frac{\partial v}{\partial y}-\frac{w}{R_2}+\frac{1}{2}(\frac{\partial w}{\partial y})^2)-B_{11}\frac{\partial^2 w}{\partial y^2}+A_{31}^e\phi\end{aligned} \tag{41}$$

$$\begin{aligned}M_{yy}&=B_{12}(\frac{\partial u}{\partial x}-\frac{w}{R_1}+\frac{1}{2}(\frac{\partial w}{\partial x})^2)-D_{12}\frac{\partial^2 w}{\partial x^2}\\&+B_{11}(\frac{\partial v}{\partial y}-\frac{w}{R_2}+\frac{1}{2}(\frac{\partial w}{\partial y})^2)-D_{11}\frac{\partial^2 w}{\partial y^2}+E_{31}^e\phi\end{aligned} \tag{42}$$

$$N_{xy}=A_{66}(\frac{\partial u}{\partial y}+\frac{\partial v}{\partial x}+\frac{\partial w}{\partial x}\frac{\partial w}{\partial y})-2B_{66}\frac{\partial^2 w}{\partial x\partial y} \tag{43}$$

$$M_{xy}=B_{66}(\frac{\partial u}{\partial y}+\frac{\partial v}{\partial x}+\frac{\partial w}{\partial x}\frac{\partial w}{\partial y})-2D_{66}\frac{\partial^2 w}{\partial x\partial y} \tag{44}$$

$$\int_{-h/2}^{h/2}D_x\, cos(\xi z)dz=+F_{11}^e\frac{\partial \phi}{\partial x} \tag{45}$$

$$\int_{-h/2}^{h/2}D_y\, cos(\xi z)dz=+F_{22}^e\frac{\partial \phi}{\partial y} \tag{46}$$

$$\begin{aligned}&\int_{-h/2}^{h/2}D_z\xi\, sin(\xi z)dz=A_{31}^e(\frac{\partial u}{\partial x}-\frac{w}{R_1}+\frac{1}{2}(\frac{\partial w}{\partial x})^2)\\&+A_{31}^e(\frac{\partial v}{\partial y}-\frac{w}{R_2}+\frac{1}{2}(\frac{\partial w}{\partial y})^2)-E_{31}^e(\frac{\partial^2 w}{\partial x^2}+\frac{\partial^2 w}{\partial y^2})-F_{33}^e\phi\end{aligned} \tag{47}$$

Moreover, the resultants associated with the double

stresses may be introduced by:

$$\begin{aligned}T_{xxx} &= Z_{11}\left(\frac{\partial^2 u}{\partial x^2}+\frac{1}{R_1}\frac{\partial w}{\partial x}+\frac{\partial w}{\partial x}\frac{\partial^2 w}{\partial x^2}\right)\\&+Z_{22}\left(\frac{\partial^2 v}{\partial x\partial y}+\frac{1}{R_2}\frac{\partial w}{\partial x}+\frac{\partial^2 w}{\partial x\partial y}\frac{\partial w}{\partial y}\right)\\&+0.5Z_{33}\left(\frac{\partial^2 u}{\partial y^2}+\frac{\partial^2 v}{\partial x\partial y}+\frac{\partial w}{\partial x}\frac{\partial^2 w}{\partial y^2}+\frac{\partial^2 w}{\partial x\partial y}\frac{\partial w}{\partial y}\right)\\&-F_{11}\frac{\partial^3 w}{\partial x^3}-(F_{22}+F_{33})\frac{\partial^3 w}{\partial x\partial y^2}\end{aligned} \tag{48}$$

$$\begin{aligned}M_{xxx} &= F_{11}\left(\frac{\partial^2 u}{\partial x^2}+\frac{1}{R_1}\frac{\partial w}{\partial x}+\frac{\partial w}{\partial x}\frac{\partial^2 w}{\partial x^2}\right)\\&+F_{22}\left(\frac{\partial^2 v}{\partial x\partial y}+\frac{1}{R_2}\frac{\partial w}{\partial x}+\frac{\partial^2 w}{\partial x\partial y}\frac{\partial w}{\partial y}\right)\\&+0.5F_{33}\left(\frac{\partial^2 u}{\partial y^2}+\frac{\partial^2 v}{\partial x\partial y}+\frac{\partial w}{\partial x}\frac{\partial^2 w}{\partial y^2}+\frac{\partial^2 w}{\partial x\partial y}\frac{\partial w}{\partial y}\right)\\&-H_{11}\frac{\partial^3 w}{\partial x^3}-(H_{22}+H_{33})\frac{\partial^3 w}{\partial x\partial y^2}\end{aligned} \tag{49}$$

$$\begin{aligned}T_{yxx} &= Z_{22}\left(\frac{\partial^2 v}{\partial y^2}+\frac{1}{R_2}\frac{\partial w}{\partial y}+\frac{\partial w}{\partial y}\frac{\partial^2 w}{\partial y^2}\right)\\&+Z_{55}\left(\frac{\partial^2 u}{\partial x\partial y}+\frac{1}{R_1}\frac{\partial w}{\partial y}+\frac{\partial^2 w}{\partial x\partial y}\frac{\partial w}{\partial x}\right)\\&+Z_{44}\left(\frac{1}{2}\left(\frac{\partial^2 u}{\partial x\partial y}+\frac{\partial^2 v}{\partial x^2}+\frac{\partial^2 w}{\partial x^2}\frac{\partial w}{\partial y}+\frac{\partial w}{\partial x}\frac{\partial^2 w}{\partial x\partial y}\right)\right)\\&-F_{22}\frac{\partial^3 w}{\partial y^3}-(F_{44}+F_{55})\frac{\partial^3 w}{\partial x^2\partial y}\end{aligned} \tag{50}$$

$$\begin{aligned}M_{yxx} &= F_{22}\left(\frac{\partial^2 v}{\partial y^2}+\frac{1}{R_2}\frac{\partial w}{\partial y}+\frac{\partial w}{\partial y}\frac{\partial^2 w}{\partial y^2}\right)\\&+F_{55}\left(\frac{\partial^2 u}{\partial x\partial y}+\frac{1}{R_1}\frac{\partial w}{\partial y}+\frac{\partial^2 w}{\partial x\partial y}\frac{\partial w}{\partial x}\right)\\&+F_{44}\left(\frac{1}{2}\left(\frac{\partial^2 u}{\partial x\partial y}+\frac{\partial^2 v}{\partial x^2}+\frac{\partial^2 w}{\partial x^2}\frac{\partial w}{\partial y}+\frac{\partial w}{\partial x}\frac{\partial^2 w}{\partial x\partial y}\right)\right)\\&-H_{22}\frac{\partial^3 w}{\partial y^3}-(H_{44}+H_{55})\frac{\partial^3 w}{\partial x^2\partial y}\end{aligned} \tag{51}$$

$$T_{zxx} = -Z_{55}\frac{\partial^2 w}{\partial x^2}-2\tilde{Z}_{22}\frac{\partial^2 w}{\partial y^2} \tag{52}$$

$$\begin{aligned}T_{xyy} &= Z_{44}\left(\frac{1}{2}\left(\frac{\partial^2 u}{\partial y^2}+\frac{\partial^2 v}{\partial x\partial y}+\frac{\partial w}{\partial x}\frac{\partial^2 w}{\partial y^2}+\frac{\partial^2 w}{\partial x\partial y}\frac{\partial w}{\partial y}\right)\right)\\&+Z_{22}\left(\frac{\partial^2 u}{\partial x^2}+\frac{1}{R_1}\frac{\partial w}{\partial x}+\frac{\partial w}{\partial x}\frac{\partial^2 w}{\partial x^2}\right)\\&+Z_{55}\left(\frac{\partial^2 v}{\partial x\partial y}+\frac{1}{R_2}\frac{\partial w}{\partial x}+\frac{\partial^2 w}{\partial x\partial y}\frac{\partial w}{\partial y}\right)\\&-(F_{44}+F_{55})\frac{\partial^3 w}{\partial x\partial y^2}-F_{22}\frac{\partial^3 w}{\partial x^3}\end{aligned} \tag{53}$$

$$\begin{aligned}M_{xyy} &= F_{44}\left(\frac{1}{2}\left(\frac{\partial^2 u}{\partial y^2}+\frac{\partial^2 v}{\partial x\partial y}+\frac{\partial w}{\partial x}\frac{\partial^2 w}{\partial y^2}+\frac{\partial^2 w}{\partial x\partial y}\frac{\partial w}{\partial y}\right)\right)\\&+F_{22}\left(\frac{\partial^2 u}{\partial x^2}+\frac{1}{R_1}\frac{\partial w}{\partial x}+\frac{\partial w}{\partial x}\frac{\partial^2 w}{\partial x^2}\right)\\&+F_{55}\left(\frac{\partial^2 v}{\partial x\partial y}+\frac{1}{R_2}\frac{\partial w}{\partial x}+\frac{\partial^2 w}{\partial x\partial y}\frac{\partial w}{\partial y}\right)\\&-(H_{44}+H_{55})\frac{\partial^3 w}{\partial x\partial y^2}-H_{22}\frac{\partial^3 w}{\partial x^3}\end{aligned} \tag{54}$$

$$\begin{aligned}T_{yyy} &= Z_{22}\left(\frac{\partial^2 u}{\partial x\partial y}+\frac{1}{R_1}\frac{\partial w}{\partial y}+\frac{\partial^2 w}{\partial x\partial y}\frac{\partial w}{\partial x}\right)\\&+Z_{33}\left(\frac{1}{2}\left(\frac{\partial^2 u}{\partial x\partial y}+\frac{\partial^2 v}{\partial x^2}+\frac{\partial^2 w}{\partial x^2}\frac{\partial w}{\partial y}+\frac{\partial w}{\partial x}\frac{\partial^2 w}{\partial x\partial y}\right)\right)\\&+Z_{11}\left(\frac{\partial^2 v}{\partial y^2}+\frac{1}{R_2}\frac{\partial w}{\partial y}+\frac{\partial w}{\partial y}\frac{\partial^2 w}{\partial y^2}\right)\\&-(F_{22}+F_{33})\frac{\partial^3 w}{\partial x^2\partial y}-F_{11}\frac{\partial^3 w}{\partial y^3}\end{aligned} \tag{55}$$

$$\begin{aligned}M_{yyy} &= F_{22}\left(\frac{\partial^2 u}{\partial x\partial y}+\frac{1}{R_1}\frac{\partial w}{\partial y}+\frac{\partial^2 w}{\partial x\partial y}\frac{\partial w}{\partial x}\right)\\&+F_{33}\left(\frac{1}{2}\left(\frac{\partial^2 u}{\partial x\partial y}+\frac{\partial^2 v}{\partial x^2}+\frac{\partial^2 w}{\partial x^2}\frac{\partial w}{\partial y}+\frac{\partial w}{\partial x}\frac{\partial^2 w}{\partial x\partial y}\right)\right)\\&+F_{11}\left(\frac{\partial^2 v}{\partial y^2}+\frac{1}{R_2}\frac{\partial w}{\partial y}+\frac{\partial w}{\partial y}\frac{\partial^2 w}{\partial y^2}\right)\\&-(H_{22}+H_{33})\frac{\partial^3 w}{\partial x^2\partial y}-H_{11}\frac{\partial^3 w}{\partial y^3}\end{aligned} \tag{56}$$

$$T_{zyy} = -2\tilde{Z}_{22}\frac{\partial^2 w}{\partial x^2}-Z_{55}\frac{\partial^2 w}{\partial y^2} \tag{57}$$

$$\begin{aligned}T_{xxy} = T_{xyx} &= 0.5Z_{33}\left(\frac{\partial^2 v}{\partial y^2}+\frac{1}{R_2}\frac{\partial w}{\partial y}+\frac{\partial w}{\partial y}\frac{\partial^2 w}{\partial y^2}\right)\\&+Z_{66}\left(\frac{1}{2}\left(\frac{\partial^2 u}{\partial x\partial y}+\frac{\partial^2 v}{\partial x^2}+\frac{\partial^2 w}{\partial x^2}\frac{\partial w}{\partial y}+\frac{\partial w}{\partial x}\frac{\partial^2 w}{\partial x\partial y}\right)\right)\\&+0.5Z_{44}\left(\frac{\partial^2 u}{\partial x\partial y}+\frac{1}{R_1}\frac{\partial w}{\partial y}+\frac{\partial^2 w}{\partial x\partial y}\frac{\partial w}{\partial x}\right)\\&-0.5F_{33}\frac{\partial^3 w}{\partial y^3}-(0.5F_{44}+F_{66})\frac{\partial^3 w}{\partial x^2\partial y}\end{aligned} \tag{58}$$

$$\begin{aligned}M_{xxy} = M_{xyx} &= 0.5F_{33}\left(\frac{\partial^2 v}{\partial y^2}+\frac{1}{R_2}\frac{\partial w}{\partial y}+\frac{\partial w}{\partial y}\frac{\partial^2 w}{\partial y^2}\right)\\&+F_{66}\left(\frac{1}{2}\left(\frac{\partial^2 u}{\partial x\partial y}+\frac{\partial^2 v}{\partial x^2}+\frac{\partial^2 w}{\partial x^2}\frac{\partial w}{\partial y}+\frac{\partial w}{\partial x}\frac{\partial^2 w}{\partial x\partial y}\right)\right)\\&+0.5F_{44}\left(\frac{\partial^2 u}{\partial x\partial y}+\frac{1}{R_1}\frac{\partial w}{\partial y}+\frac{\partial^2 w}{\partial x\partial y}\frac{\partial w}{\partial x}\right)\\&-0.5H_{33}\frac{\partial^3 w}{\partial y^3}-(0.5H_{44}+H_{66})\frac{\partial^3 w}{\partial x^2\partial y}\end{aligned} \tag{59}$$

$$\begin{aligned}T_{yxy} = T_{yyx} &= 0.5Z_{44}\left(\frac{\partial^2 v}{\partial x\partial y}+\frac{1}{R_2}\frac{\partial w}{\partial x}+\frac{\partial^2 w}{\partial x\partial y}\frac{\partial w}{\partial y}\right)\\&+0.5Z_{33}\left(\frac{\partial^2 u}{\partial x^2}+\frac{1}{R_1}\frac{\partial w}{\partial x}+\frac{\partial w}{\partial x}\frac{\partial^2 w}{\partial x^2}\right)\\&+Z_{66}\left(\frac{1}{2}\left(\frac{\partial^2 u}{\partial y^2}+\frac{\partial^2 v}{\partial x\partial y}+\frac{\partial w}{\partial x}\frac{\partial^2 w}{\partial y^2}+\frac{\partial^2 w}{\partial x\partial y}\frac{\partial w}{\partial y}\right)\right)\\&-(0.5F_{44}+F_{66})\frac{\partial^3 w}{\partial x\partial y^2}-0.5F_{33}\frac{\partial^3 w}{\partial x^3}\end{aligned} \tag{60}$$

$$M_{yxy} = M_{yyx} = 0.5F_{44}(\frac{\partial^2 v}{\partial x \partial y} + \frac{1}{R_2}\frac{\partial w}{\partial x} + \frac{\partial^2 w}{\partial x \partial y}\frac{\partial w}{\partial y}) + 0.5F_{33}(\frac{\partial^2 u}{\partial x^2} + \frac{1}{R_1}\frac{\partial w}{\partial x} + \frac{\partial w}{\partial x}\frac{\partial^2 w}{\partial x^2}) + F_{66}(\frac{1}{2}(\frac{\partial^2 u}{\partial y^2} + \frac{\partial^2 v}{\partial x \partial y} + \frac{\partial w}{\partial x}\frac{\partial^2 w}{\partial y^2} + \frac{\partial^2 w}{\partial x \partial y}\frac{\partial w}{\partial y})) - (0.5H_{44} + H_{66})\frac{\partial^3 w}{\partial x \partial y^2} - 0.5H_{33}\frac{\partial^3 w}{\partial x^3} \quad (61)$$

$$T_{zxy} = T_{zyx} = -2\tilde{Z}_{44}\frac{\partial^2 w}{\partial x \partial y} \quad (62)$$

so that

$$\{A_{11}, B_{11}, D_{11}\} = \int_{-h/2}^{h/2} \tilde{C}_{11}\{1, z, z^2\}dz, \quad (63)$$

$$\{A_{12}, B_{12}, D_{12}\} = \int_{-h/2}^{h/2} \tilde{C}_{12}\{1, z, z^2\}dz, \quad (64)$$

$$\{A_{66}, B_{66}, D_{66}\} = \int_{-h/2}^{h/2} \tilde{C}_{66}\{1, z, z^2\}dz, \quad (65)$$

$$\{A_{31}^e, E_{31}^e\} = \int_{-h/2}^{h/2} \tilde{e}_{31}\xi\, sin(\xi z)\{1, z\}\, dz \quad (66)$$

$$\{F_{11}^e, F_{22}^e, F_{33}^e\} = \int_{-h/2}^{h/2} \begin{Bmatrix} \tilde{k}_{11}\, cos^2(\xi z), \tilde{k}_{22}\, cos^2(\xi z), \\ \tilde{k}_{33}\xi^2\, sin^2(\xi z) \end{Bmatrix} dz \quad (67)$$

$$\{Z_{11}, Z_{22}, Z_{33}, Z_{44}, Z_{55}, Z_{66}\} = \int_{-h/2}^{h/2} \{\beta_1, \beta_2, \beta_3, \beta_4, \beta_5, \beta_6\}dz \quad (68)$$

$$\{F_{11}, F_{22}, F_{33}, F_{44}, F_{55}, F_{66}\} = \int_{-h/2}^{h/2} \{\beta_1, \beta_2, \beta_3, \beta_4, \beta_5, \beta_6\}zdz \quad (69)$$

$$\{H_{11}, H_{22}, H_{33}, H_{44}, H_{55}, H_{66}\} = \int_{-h/2}^{h/2} \{\beta_1, \beta_2, \beta_3, \beta_4, \beta_5, \beta_6\}z^2 dz \quad (70)$$

$$\{\tilde{Z}_{22}, \tilde{Z}_{44}\} = \int_{-h/2}^{h/2} \{a_2, a_4\}dz \quad (71)$$

5. Method of solution

Based on Galerkin's method, it is possible to provide a solution for vibration problem of piezo-electric microshells based on the boundary conditions:

$$\phi = 0 \qquad \text{on electrical displacement} \quad (72)$$

$$w = \frac{\partial^2 w}{\partial x^2} = 0 \qquad \text{on deflection} \quad (73)$$

In next step, the four variables based on thin piezo-electric shell model can be defined by:

$$u = \sum_{r=1}^{\infty}\sum_{p=1}^{\infty} U_{rp}\bar{u}(x, y) = \sum_{r=1}^{\infty}\sum_{p=1}^{\infty} U_{rp}\frac{\partial G_r(x)}{\partial x}G_p(y) \quad (74)$$

$$v = \sum_{r=1}^{\infty}\sum_{p=1}^{\infty} V_{rp}\bar{v}(x, y) = \sum_{r=1}^{\infty}\sum_{p=1}^{\infty} V_{rp}G_r(x)\frac{\partial G_p(y)}{\partial y} \quad (75)$$

$$w = \sum_{r=1}^{\infty}\sum_{p=1}^{\infty} W_{rp}\bar{w}(x, y) = \sum_{r=1}^{\infty}\sum_{p=1}^{\infty} W_{rp}G_r(x)\, G_p(y) \quad (76)$$

$$\phi = \sum_{r=1}^{\infty}\sum_{p=1}^{\infty} \Phi_{rp}\bar{\phi}(x, y) = \sum_{r=1}^{\infty}\sum_{p=1}^{\infty} \Phi_{rp}G_r(x)\, G_p(y) \quad (77)$$

In this research, the vibrational amplitudes have been denoted by U_{rp}, V_{rp}, W_{rp} and Φ_{rp}. Two functions $G_m = sin(\frac{r\pi}{L}x)$ and $\boldsymbol{G_n = sin(\frac{p\pi}{b}y)}$ for simply-supported edges are chosen to satisfy the boundary conditions. Pursuant to the method of Galerkin and insertion of displacements represented as Eqs. (74)-(77) in the governing equations, each of equations may be exhibited as residual R_i (i = 1, 2, 3, 4) leading to:

$$\int_0^b\int_0^L \sum_{m=1}^{\infty}\sum_{n=1}^{\infty} \bar{u}(x, y)\, R_1 = 0 \quad (78)$$

$$\int_0^b\int_0^L \sum_{m=1}^{\infty}\sum_{n=1}^{\infty} \bar{v}(x, y)\, R_2 = 0 \quad (79)$$

$$\int_0^b\int_0^L \sum_{m=1}^{\infty}\sum_{n=1}^{\infty} \bar{w}(x, y)\, R_3 = 0 \quad (80)$$

$$\int_0^b\int_0^L \sum_{m=1}^{\infty}\sum_{n=1}^{\infty} \bar{\phi}(x, y)\, R_4 = 0 \quad (81)$$

The above procedure leads to the below ordinary equations of having nonlinear terms as:

$$k_{11}U + k_{21}V + k_{31}W + g_1W^2 + k_{41}\Phi = 0 \quad (82)$$

$$k_{12}U + k_{22}V + k_{32}W + g_2W^2 + k_{42}\Phi = 0 \quad (83)$$

$$M\ddot{W} + k_{13}U + k_{23}V + k_{33}W + g_3W^2 + g_4W^3 + g_5UW + g_6VW + k_{43}\Phi + g_7\Phi W = 0 \quad (84)$$

$$k_{14}U + k_{24}V + k_{34}W + g_8W^2 + k_{44}\Phi = 0 \quad (85)$$

Note that g_i and k_{ij} are the components of nonlinear and linear stiffness matrices. Owning to the reason that there are four coupled nonlinear governing equations, providing the closed-form frequency as a function of maximum amplitude

(W) is very hard. Thus, by simultaneous solve of Eqs. (82), (83), and (85), it is feasible to calculate amplitudes (U, V, Φ) as functions of transverse amplitude or maximum deflection (W). Next, calculated amplitudes ($\hat{U}$, $\hat{V}$, $\hat{\Phi}$) have been placed in Eq. (84) in order to find a single nonlinear governing equation for microshell as:

$$\ddot{W} + \frac{K_1}{M}W + \frac{K_2}{M}W|W| + \frac{K_3}{M}W^3 = 0 \tag{87}$$

By simplifying the obtained equation, the above equation may be obtained as:

It must be pointed out that K_1, K_2 and K_3 have complex forms and expressing their closed forms is very difficult. According to the primary conditions $W = \bar{W}, \dot{W} = 0$ at t = 0, the solution of Eq. (87) may be assumed with the use of trigonometric function as:

$$W = \bar{W}\, cos(\omega_{NL} t) \tag{88}$$

where ω_{NL} exhibits the nonlinear vibration frequency. Finally, the nonlinear vibrational frequency can be expressed by (Barati and Shahverdi 2018b):

$$\omega_{NL} = \sqrt{\frac{K_1}{M} + \frac{8\bar{W}}{3\pi}\frac{K_2}{M} + \frac{3}{4}\frac{K_3}{M}(\bar{W})^2} \tag{89}$$

To present obtained results, non-dimension frequency and deflection can be defined by:

$$\varpi = 10\omega_{NL}L\sqrt{\frac{\rho^u}{C_{11}^u}}, \widetilde{W} = \frac{\bar{W}}{h} \tag{90}$$

6. Results and discussions

In this chapter, impacts of different factors such as electrical field, three scale coefficients, curvature radius and material compositions on nonlinear vibrational frequencies of doubly-curved MEE microshells have been examined. The thickness of micro-sized shell has been chosen to be h = 10 μm. The values of scale coefficients have been selected in range of $0 < l_0 = l_1 = l_2 < 0.5$ has used in former researches (Mirjavadi *et al*. 2020b). Table 1 represents the material properties of the two phases of composite piezoelectric material.

For the case of micro-scaled isotropic cylindrical shells formulated via MSGT, the frequencies reported by Zeyghampour and Beni (2014) have been re-calculated in this article and the comparison has been presented in Table 2. The scale coefficients in Table 2 have been chosen as $l_0 = l_1 = l_2 = 0$ and $l_0 = l_1 = l_2 = h$ when the microshell dimension is h/R = 0.02 and h/R = 0.05. Further verification has been presented via the comparison of the nonlinear vibrational frequencies of piezoelectric shells with those of Mirjavadi *et al*. (2020b), as indicated in Fig. 2. For the figure, it has been considered that L/R = 2, R/h = 100.

Fig. 3 exhibits the changing of non-dimensional vibrational frequency of multi-phase doubly-curvature microshells with respect to normalized amplitude, based on diverse scale coefficients (l_0, l_1, l_2) assuming V_E = 0 and R = 7L. For ease of investigation, it has been selected that $l_0 = l_1 = l_2$. The piezoelectric phase percentage is selected to be V_f = 20%. The first intuition is that the vibrational frequency initially declines by the addition of normalized amplitude ($\widetilde{W}$). Subsequently, the vibrational frequency starts to be increased at high values of $\widetilde{W}$. It should be elucidated that the frequency has been named linear vibrational frequency when $\widetilde{W} = 0$ and it is named nonlinear vibrational frequency when $\widetilde{W} > 0$. It can be understood that non-dimensional vibration frequency of doubly-curvature micro-scaled shells is often greater than that of macro-scale shells for which $l_0 = l_1 = l_2 = 0$. The non-dimensional frequency increases via increasing in the strain gradient coefficients. This finding is owning to the fact that the impression of micro scale, that describes the reciprocal impacts of each point inside the region, may improve the strength of structures.

An analogy among the calculated frequencies according

Table 1 Material properties of two-phase piezo-electrics made of $BaTiO_3$-$CoFe_2O_4$

Property	V_f = 0	V_f = 0.2	V_f = 0.4	V_f = 0.6	V_f = 0.8
C_{11} *(GPa)*	286	250	225	200	175
C_{13}	170	145	125	110	100
C_{33}	269.5	240	220	190	170
e_{31} *(C/m²)*	0	-2	-3	-3.5	-4
e_{33}	0	4	7	11	14
k_{11} *(10^{-9} C/Vm)*	0.08	0.33	0.8	0.9	1
k_{33}	0.093	2.5	5	7.5	10

Table 2 Comparing the of natural frequencies of microshells using MSGT (L/R = 5)

h/R	$l_0 = l_1 = l_2 = 0$		$l_0 = l_1 = l_2 = h$	
	Zeighampour and Beni 2014	present	Zeighampour and Beni 2014	present
0.02	0.19543	0.19544	0.19801	0.19802
0.05	0.19588	0.19588	0.21109	0.21109

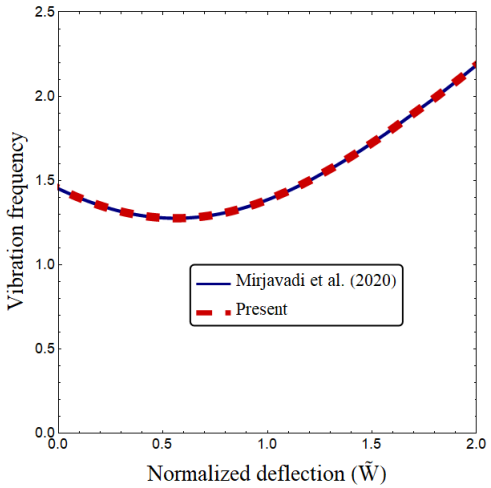

Fig. 2 Vibrational frequency validation of a smart piezo-electric shell (L/R = 2, R/h = 100, VE = 0)

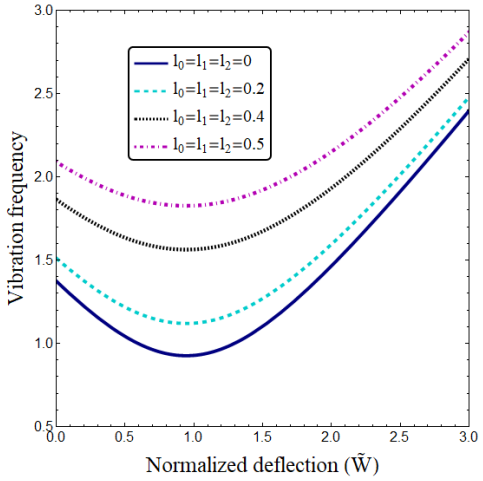

Fig. 3 Dimensionless frequency of doubly-curved micro-shells versus non-dimension deflection according to different scale parameters (R = 7L, L = 50h, V_E = 0, V_f = 20%)

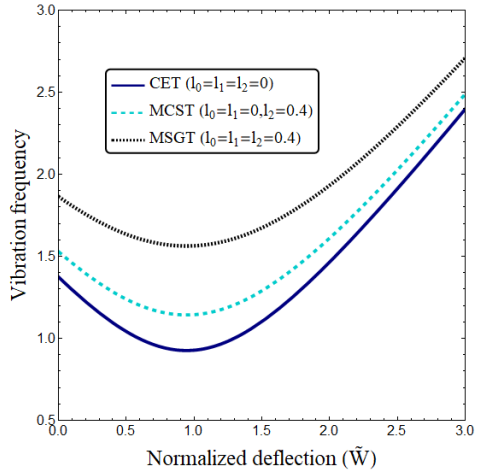

Fig. 4 Dimensionless frequency of doubly-curved micro-shells versus non-dimension deflection according to different elasticity theories (R = 7L, L = 50h, V_E = 0, V_f = 20%)

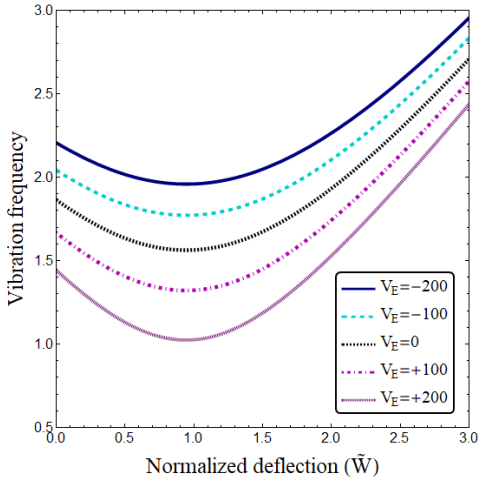

Fig. 5 Dimensionless frequency of doubly-curved micro-shells versus non-dimension deflection according to different voltages (R = 7L, l_0 = l_1 = l_2 = 0.4h, L = 50h, V_f = 20%)

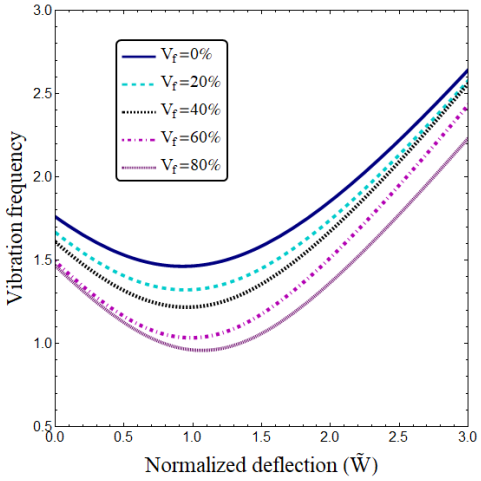

(a) V_E = +100

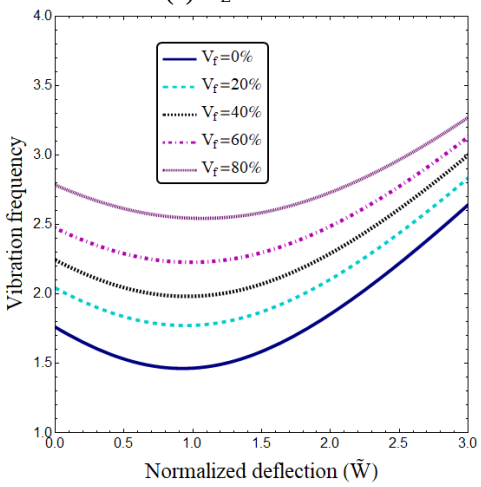

(b) V_E = -100

Fig. 6 Dimensionless frequency of doubly-curved micro-shells versus non-dimension deflection according to different piezoelectric volume fraction (R = 7L, l_0 = l_1 = l_2 = 0.4h, L = 50h)

to various elasticity theories containing CET with l_0 = l_1 = l_2 = 0, MCST with l_0 = l_1 = 0, l_2 = 0.4h and MSGT with l_0 = l_1 = l_2 = 0.4h has been exhibited in Fig. 4. The smallest frequency value has been achieved according to CET in which no scale coefficient is present. The frequency value according to MCST is smaller than that of MSGT. This is owning to the fact that MCST has only one scale coefficient and the impressions of dilatation gradient and deviatoric stretch gradient have been discarded.

In Fig. 5, changing of non-dimension vibration frequency of doubly-curved piezoelectric microshell versus non-dimension amplitude is illustrated for different electrical voltages when L = 50h and V_f = 20%. This is deduced that non-dimension vibration frequencies of doubly-curved piezoelectric micro-size shell are significantly influenced by the magnitude and sign of electric potentials for each values of non-dimension amplitude. It is concluded that smaller magnitudes of electrical voltages result in greater vibration frequency. Actually, the imposed positive/negative electrical fields might generate the in-plane compressive and tensile forces. It is also found that

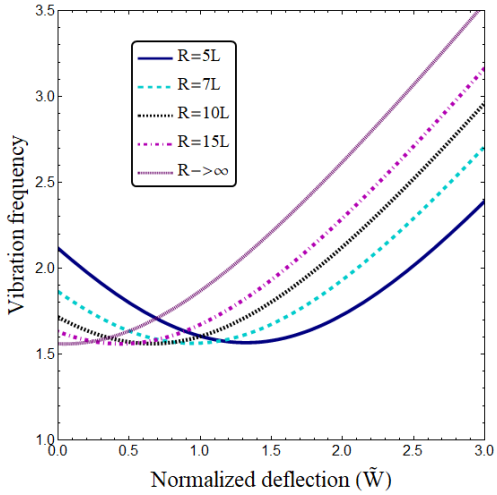

Fig. 7 Dimensionless frequency of doubly-curved micro-shells versus non-dimension deflection according to different curvature radius (V_f = 20%, $l_0 = l_1 = l_2$ = 0.4h, L = 50h, V_E = 0)

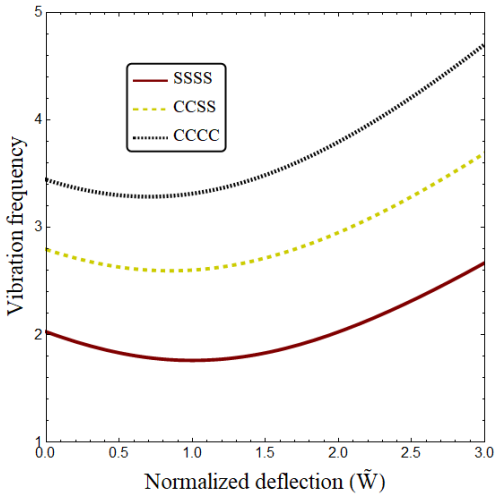

Fig. 8 Vibration frequency of FGP doubly-curved micro-shell against normalized deflection based on different boundary conditions ($l_0 = l_1 = l_2$ = 0.4h, L = 50h, V_E = 0)

the vibration frequency begins to decline with the increase of non-dimension amplitude. Next, the vibration frequency begins to increase at larger values of non-dimension amplitude.

Fig. 6 depicts the variation of vibration frequency against normalized amplitude accounting for various percentages of piezoelectric ingredient (V_f = 0, 20%, 40%, 60% and 80%). For simplicity, the scale factors are selected to be $l_0 = l_1 = l_2$ = 0.4h. The applied electric voltage is chosen as V_E = -100 V and V_E = +100 V. It is realized that the highest frequency at V_E = +100 V occurs for zero piezo-electric phase percentage V_f = 0. But, the highest frequency at V_E = -100 V occurs for piezoelectric phase percentage V_f 80%. This observation is associated with the negative value of piezoelectric constant (e_{31}) as presented in Table 1. Therefore, the material composition in multi-phase piezoelectric material has a key role in vibration analysis of micro-scale shells

Non-dimension frequency against normalized deflection of the microshell accounting for various curvature radius has been exhibited in Fig. 7. Note that an infinite curvature radius results in frequency curves for flat plates. So, as the value of curvature has been reduced, the curvature radius has more announced effect on frequency curves.

In Fig. 8, the frequency results for a doubly-curved micro-size shell according to diverse boundary conditions have been presented. The assumed boundary conditions are: SSSS, CCSS and CCCC. Consider that SSSS refers to fully simply-supported boundary conditions and CCCC refers to fully clamped boundary conditions. As expected inclusion of clamped edge conditions leads to a stiffer micro-size shell and higher vibration frequencies.

7. Conclusions

Vibration characteristics of a piezo-electric microshell with double curvature were reported in the present article. The complete formulation and solution for the problem based on thin shell model was presented. This was reported that the vibration behavior of the micro-sized shell is sensitive to material composition. There was a notable change in vibration frequency versus applied voltage when the piezoelectric volume fraction was changed. Also, applying positive or negative electrical potentials led to increasing or reducing the vibration frequency. Another observation was that size effects due to strain gradients changed significantly the vibration behaviors of piezo-electric micro-sized shell. Also, as the value of curvature was reduced, the curvature radius had more announced effect on frequency curves.

References

Abdulrazzaq, M.A., Muhammad, A.K., Kadhim, Z.D. and Faleh, N.M. (2020), "Vibration analysis of nonlocal strain gradient porous FG composite plates coupled by visco-elastic foundation based on DQM", *Coupled Syst. Mech.*, **9**(3), 201-217. https://doi.org/10.12989/csm.2020.9.3.201.

Aboudi, J. (2001), "Micromechanical analysis of fully coupled electro-magneto-thermo-elastic multiphase composites", *Smart Mater. Struct.*, **10**(5), 867. https://doi.org/10.1088/0964-1726/10/5/303.

Ahmed, R.A., Fenjan, R.M., Hamad, L.B. and Faleh, N.M. (2020a), "A review of effects of partial dynamic loading on dynamic response of nonlocal functionally graded material beams", *Adv. Mater. Res.*, **9**(1), 33-48. https://doi.org/10.12989/amr.2020.9.1.033.

Ahmed, R.A., Al-Maliki, A.F. and Faleh, N.M. (2020b), "Dynamic characteristics of multi-phase crystalline porous shells with using strain gradient elasticity", *Adv. Nano Res.*, **8**(2), 157-167. https://doi.org/10.12989/anr.2020.8.2.157.

Al-Maliki, A.F., Faleh, N.M. and Alasadi, A.A. (2019), "Finite element formulation and vibration of nonlocal refined metal foam beams with symmetric and non-symmetric porosities", *Struct. Monitor. Maint.*, **6**(2), 147-159. https://doi.org/10.12989/smm.2019.6.2.147.

Annigeri, A.R., Ganesan, N. and Swarnamani, S. (2007), "Free vibration behaviour of multiphase and layered magneto-electro-elastic beam", *J. Sound Vib.*, **299**(1-2), 44-63.

https://doi.org/10.1016/j.jsv.2006.06.044.
Barati, M.R. (2017), "Magneto-hygro-thermal vibration behavior of elastically coupled nanoplate systems incorporating nonlocal and strain gradient effects", *J. Braz. Soc. Mech. Sci. Eng.*, **39**(11), 4335-4352. https://doi.org/10.1007/s40430-017-0890-x.
Barati, M.R. (2018a), "Nonlocal stress-strain gradient vibration analysis of heterogeneous double-layered plates under hygro-thermal and linearly varying in-plane loads", *J. Vib. Control*, **24**(19), 4630-4647. https://doi.org/10.1177%2F1077546317731672.
Barati, M.R. (2018b), "Porosity-dependent vibration and dynamic stability of compositionally gradient nanofilms using nonlocal strain gradient theory", *Proceedings of the Institution of Mechanical Engineers, Part C: Journal of Mechanical Engineering Science*, **232**(17), 3144-3155. https://doi.org/10.1177%2F0954406217729421.
Barati, M.R. (2018c), "Temperature and porosity effects on wave propagation in nanobeams using bi-Helmholtz nonlocal strain-gradient elasticity", *Eur. Phys. J. Plus*, **133**(5), 170. https://doi.org/10.1140/epjp/i2018-11993-0.
Barati, M.R. and Shahverdi, H. (2018a), "Forced vibration of porous functionally graded nanoplates under uniform dynamic load using general nonlocal stress–strain gradient theory", *J. Vib. Control*, **24**(20), 4700-4715. https://doi.org/10.1177%2F1077546317733832.
Barati, M.R. and Shahverdi, H. (2018b), "Nonlinear thermal vibration analysis of refined shear deformable FG nanoplates: two semi-analytical solutions", *J. Braz. Soc. Mech. Sci. Eng.*, **40**(2), 1-15. https://doi.org/10.1007/s40430-018-0968-0.
Chen, R., Cheng, Y., Wang, P., Wang, Y., Wang, Q., Yang, Z. and Su, C. (2021), "Facile synthesis of a sandwiched $Ti_3C_2T_x$ MXene/nZVI/fungal hypha nanofiber hybrid membrane for enhanced removal of Be (II) from $Be(NH_2)_2$ complexing solutions", *Chemical Engineering Journal*, **421**, 129682. https://doi.org/10.1016/j.cej.2021.129682.
Deng, X., Xu, T., Huang, G., Li, Q., Luo, L., Zhao, Y. and Zhu, B. (2020), "Design and fabrication of a novel dual-frequency confocal ultrasound transducer for microvessels super-harmonic Iimaging", *IEEE T. Ultrasonics Ferroelectrics Freq. Control*, **68**(4), 1272-1277. https://doi.org/10.1109/TUFFC.2020.3028505.
Deng, R., Li, M. and Linghu, S. (2021), "Sensitivity analysis of steam injection parameters of steam injection thermal recovery technology", *Fresenius Environ. Bull.*, **30**(5), 5385-5394.
Duan, X., Xu, Z., Sun, X., Deng, B. and Liu, J. (2021), "ffects of injection timing and EGR on combustion and emissions characteristics of the diesel engine fuelled with acetone–butanol–ethanol/diesel blend fuels", *Energy*, **231**, 121069. https://doi.org/10.1016/j.energy.2021.121069.
Ebrahimi, F. and Barati, M.R. (2017), "Dynamic modeling of preloaded size-dependent nano-crystalline nano-structures", *Appl. Math. Mech.*, **38**(12), 1753-1772. https://doi.org/10.1007/s10483-017-2291-8.
Ebrahimi, F. and Barati, M.R. (2018a), "Free vibration analysis of couple stress rotating nanobeams with surface effect under in-plane axial magnetic field", *J. Vib. Control*, **24**(21), 5097-5107. https://doi.org/10.1177%2F1077546317744719.
Ebrahimi, F. and Barati, M.R. (2018b), "Vibration analysis of nonlocal strain gradient embedded single-layer graphene sheets under nonuniform in-plane loads", *J. Vib. Control*, **24**(20), 4751-4763. https://doi.org/10.1177%2F1077546317734083.
Ebrahimi, F. and Barati, M.R. (2018c), "Hygro-thermal vibration analysis of bilayer graphene sheet system via nonlocal strain gradient plate theory", *J. Braz. Soc. Mech. Sci. Eng.*, **40**(9), 1-15. https://doi.org/10.1007/s40430-018-1350-y.
Ebrahimi, F. and Barati, M.R. (2018d), "Static stability analysis of double-layer graphene sheet system in hygro-thermal environment", *Microsyst. Technol.*, **24**(9), 3713-3727. https://doi.org/10.1007/s00542-018-3827-0.
Ebrahimi, F. and Barati, M.R. (2018e), "Influence of neutral surface position on dynamic characteristics of in-homogeneous piezo-magnetically actuated nanoscale plates", *Proceedings of the Institution of Mechanical Engineers, Part C: Journal of Mechanical Engineering Science*, **232**(17), 3125-3143. https://doi.org/10.1177%2F0954406217728977.
Ebrahimi, F. and Barati, M.R. (2018f), "Vibration analysis of parabolic shear-deformable piezoelectrically actuated nanoscale beams incorporating thermal effects", *Mech. Adv. Mater. Struct.*, **25**(11), 917-929. https://doi.org/10.1080/15376494.2017.1323141.
Ebrahimi, F. and Barati, M.R. (2018g), "Nonlocal and surface effects on vibration behavior of axially loaded flexoelectric nanobeams subjected to in-plane magnetic field", *Arab. J. Sci. Eng.*, **43**(3), 1423-1433. https://doi.org/10.1007/s13369-017-2943-y.
Ebrahimi, F. and Barati, M.R. (2018h), "Size-dependent thermally affected wave propagation analysis in nonlocal strain gradient functionally graded nanoplates via a quasi-3D plate theory", *Proceedings of the Institution of Mechanical Engineers, Part C: Journal of Mechanical Engineering Science*, **232**(1), 162-173. https://doi.org/10.1177%2F0954406216674243.
Eltaher, M.A., Emam, S.A. and Mahmoud, F.F. (2012), "Free vibration analysis of functionally graded size-dependent nanobeams", *Appl. Math. Computat.*, **218**(14), 7406-7420. https://doi.org/10.1016/j.amc.2011.12.090.
Eringen, A.C. (1972), "Linear theory of nonlocal elasticity and dispersion of plane waves", *Int. J. Eng. Sci.*, **10**(5), 425-435. https://doi.org/10.1016/0020-7225(72)90050-X.
Fenjan, R.M., Ahmed, R.A., Hamad, L.B. and Faleh, N.M. (2020a), "A review of numerical approach for dynamic response of strain gradient metal foam shells under constant velocity moving loads", *Adv. Computat. Des.*, **5**(4), 349-362. https://doi.org/10.12989/acd.2020.5.4.349.
Fenjan, R.M., Faleh, N.M. and Ridha, A.A. (2020b), "Strain gradient based static stability analysis of composite crystalline shell structures having porosities", *Steel Compos. Struct.*, **36**(6), 631-642. https://doi.org/10.12989/scs.2020.36.6.631.
Feng, S., Zuo, C., Zhang, L., Yin, W. and Chen, Q. (2021), "Generalized framework for non-sinusoidal fringe analysis using deep learning", *Photonic Res.*, **9**(6), 1084-1098. https://doi.org/10.1364/PRJ.420944.
Guo, J., Chen, J. and Pan, E. (2016), "Static deformation of anisotropic layered magnetoelectroelastic plates based on modified couple-stress theory", *Compos. Part B Eng.*, **107**, 84-96. https://doi.org/10.1016/j.compositesb.2016.09.044.
Huang, Z.Q., Yi, S.H., Chen, H.X. and He, X.Q. (2021), "Parameter analysis of damaged region for laminates with matrix defects", *J. Sandw. Struct. Mater.*, **23**(2), 580-620. https://doi.org/10.1177%2F1099636219842290.
Jiang, T., Liu, Z., Wang, G. and Chen, Z. (2021), "Comparative study of thermally stratified tank using different heat transfer materials for concentrated solar power plant", *Energy Rep.*, **7**, 3678-3687. https://doi.org/10.1016/j.egyr.2021.06.021.
Kordestani, H., Zhang, C., Masri, S.F. and Shadabfar, M. (2021), "An empirical time-domain trend line-based bridge signal decomposing algorithm using Savitzky–Golay filter", *Struct. Control Health Monit.*, **28**(7), e2750. https://doi.org/10.1002/stc.2750.
Kumaravel, A., Ganesan, N. and Sethuraman, R. (2007), "Buckling and vibration analysis of layered and multiphase magneto-electro-elastic beam under thermal environment", *Multidiscip. Model. Mater. Struct.*, **3**(4), 461-476. https://doi.org/10.1163/157361107782106401.
Kunbar, L.A.H., Hamad, L.B., Ahmed, R.A. and Faleh, N.M.

(2020), "Nonlinear vibration of smart nonlocal magneto-electro-elastic beams resting on nonlinear elastic substrate with geometrical imperfection and various piezoelectric effects", *Smart Struct. Syst.*, **25**(5), 619-630. https://doi.org/10.12989/sss.2020.25.5.619.

Li, Y. and Shi, Z. (2009), "Free vibration of a functionally graded piezoelectric beam via state-space based differential quadrature", *Compos. Struct.*, **87**(3), 257-264. https://doi.org/10.1016/j.compstruct.2008.01.012.

Li, Y.S. and Pan, E.S. (2015), "Static bending and free vibration of a functionally graded piezoelectric microplate based on the modified couple-stress theory", *Int. J. Eng. Sci.*, **97**, 40-59. https://doi.org/10.1016/j.ijengsci.2015.08.009.

Lou, J., He, L., Du, J. and Wu, H. (2016), "Buckling and post-buckling analyses of piezoelectric hybrid microplates subject to thermo–electro-mechanical loads based on the modified couple stress theory", *Compos. Struct.*, **153**, 332-344. https://doi.org/10.1016/j.compstruct.2016.05.107.

Lv, Z., Lou, R. and Singh, A.K. (2020a), "AI empowered communication systems for intelligent transportation systems", *IEEE T. Intell. Transp.*, **22**(7). https://doi.org/10.1109/TITS.2020.3017183.

Lv, Z., Chen, D. and Wang, Q. (2020b), "Diversified technologies in internet of vehicles under intelligent edge computing", *IEEE T. Intell. Transp.*, **22**(4), 2048-2059. https://doi.org/10.1109/TITS.2020.3019756.

Lv, S. and Liu, Y. (2021), "PLVA: privacy-preserving and lightweight V2I authentication protocol", *IEEE T. Intell. Transp.* https://doi.org/10.1109/TITS.2021.3059638.

Mirjavadi, S.S., Forsat, M., Badnava, S. and Barati, M.R. (2020a), "Analyzing nonlocal nonlinear vibrations of two-phase geometrically imperfect piezo-magnetic beams considering piezoelectric reinforcement scheme", *J. Strain Anal. Eng*, **55**(7-8), 258-270. https://doi.org/10.1177%2F0309324720917285.

Mirjavadi, S.S., Forsat, M., Badnava, S., Barati, M.R. and Hamouda, A.M.S. (2020b), "Nonlinear dynamic characteristics of nonlocal multi-phase magneto-electro-elastic nano-tubes with different piezoelectric constituents", *Appl. Phys. A*, **126**(8), 1-16. https://doi.org/10.1007/s00339-020-03743-8.

Mirjavadi, S.S., Bayani, H., Khoshtinat, N., Forsat, M., Barati, M. R. and Hamouda, A.M.S. (2020c), "On nonlinear vibration behavior of piezo-magnetic doubly-curved nanoshells", *Smart Struct. Syst.*, **26**(5), 631-640. https://doi.org/10.12989/sss.2020.26.5.631.

Mirjavadi, S.S., Forsat, M., Yahya, Y.Z., Barati, M.R., Jayasimha, A.N. and Hamouda, A.M.S. (2020d), "Porosity effects on post-buckling behavior of geometrically imperfect metal foam doubly-curved shells with stiffeners", *Struct. Eng. Mech.*, **75**(6), 701-711. https://doi.org/10.12989/sem.2020.75.6.701.

Mirjavadi, S.S., Forsat, M., Mollaee, S., Barati, M.R., Afshari, B. M. and Hamouda, A.M.S. (2020e), "Post-buckling analysis of geometrically imperfect nanoparticle reinforced annular sector plates under radial compression", *Comput. Concrete*, **26**(1), 21-30. https://doi.org/10.12989/cac.2020.26.1.021.

Mirjavadi, S.S., Nikookar, M., Mollaee, S., Forsat, M., Barati, M.R. and Hamouda, A.M.S. (2020f), "Analyzing exact nonlinear forced vibrations of two-phase magneto-electro-elastic nanobeams under an elliptic-type force", *Adv. Nano Res.*, **9**(1), 47-58. https://doi.org/10.12989/anr.2020.9.1.047.

Mirjavadi, S.S., Forsat, M., Barati, M.R. and Hamouda, A.M.S. (2020g), "Investigating nonlinear forced vibration behavior of multi-phase nanocomposite annular sector plates using Jacobi elliptic functions", *Steel Compos. Struct.*, **36**(1), 87-101. https://doi.org/10.12989/scs.2020.36.1.087.

Mirjavadi, S.S., Forsat, M., Barati, M.R. and Hamouda, A.M.S. (2020h), "Post-buckling analysis of geometrically imperfect tapered curved micro-panels made of graphene oxide powder reinforced composite", *Steel Compos. Struct.*, **36**(1), 63-74. https://doi.org/10.12989/scs.2020.36.1.063.

Mirjavadi, S.S., Forsat, M., Barati, M.R. and Hamouda, A.M.S. (2020i), "Assessment of transient vibrations of graphene oxide reinforced plates under pulse loads using finite strip method", *Comput. Concrete*, **25**(6), 575-585. https://doi.org/10.12989/cac.2020.25.6.575.

Mirjavadi, S.S., Forsat, M., Barati, M.R. and Hamouda, A.M.S. (2020j), "Post-buckling of higher-order stiffened metal foam curved shells with porosity distributions and geometrical imperfection", *Steel Compos. Struct.*, **35**(4), 567-578. https://doi.org/10.12989/scs.2020.35.4.567.

Mirjavadi, S.S., Forsat, M., Yahya, Y.Z., Barati, M.R., Jayasimha, A.N. and Khan, I. (2020k), "Analysis of post-buckling of higher-order graphene oxide reinforced concrete plates with geometrical imperfection", *Adv. Concrete Constr.*, **9**(4), 397-406. https://doi.org/10.12989/acc.2020.9.4.397.

Mirjavadi, S.S., Forsat, M., Nia, A.F., Badnava, S. and Hamouda, A.M.S. (2020l), "Nonlocal strain gradient effects on forced vibrations of porous FG cylindrical nanoshells", *Adv. Nano Res.*, **8**(2), 149-156. https://doi.org/10.12989/anr.2020.8.2.149.

Pan, E. and Han, F. (2005), "Exact solution for functionally graded and layered magneto-electro-elastic plates", *Int. J. Eng. Sci.*, **43**(3-4), 321-339. https://doi.org/10.1016/j.ijengsci.2004.09.006.

Shariati, A., Barati, M.R., Ebrahimi, F., Singhal, A. and Toghroli, A. (2020a), "Investigating vibrational behavior of graphene sheets under linearly varying in-plane bending load based on the nonlocal strain gradient theory", *Adv. Nano Res.*, **8**(4), 265-276. https://doi.org/10.12989/anr.2020.8.4.265.

Shariati, A., Barati, M.R., Ebrahimi, F. and Toghroli, A. (2020b), "Investigation of microstructure and surface effects on vibrational characteristics of nanobeams based on nonlocal couple stress theory", *Adv. Nano Res.*, **8**(3), 191-202. https://doi.org/10.12989/anr.2020.8.3.191.

Thai, H.T. and Vo, T.P. (2012), "A nonlocal sinusoidal shear deformation beam theory with application to bending, buckling, and vibration of nanobeams", *Int. J. Eng. Sci.*, **54**, 58-66. https://doi.org/10.1016/j.ijengsci.2012.01.009.

Wang, L., Liu, H. T., Ni, Q. and Wu, Y. (2013), "Flexural vibrations of microscale pipes conveying fluid by considering the size effects of micro-flow and micro-structure", *Int. J. Eng. Sci.*, **71**, 92-101. https://doi.org/10.1016/j.ijengsci.2013.06.006.

Wang, L., Peng, Y., Xie, Y., Chen, B. and Du, Y. (2021), "A new iteration regularization method for dynamic load identification of stochastic structures", *Mech. Syst. Signal Pr.*, **156**, 107586. https://doi.org/10.1016/j.ymssp.2020.107586.

Xu, X., Karami, B. and Shahsavari, D. (2021), "Time-dependent behavior of porous curved nanobeam", *Int. J. Eng. Sci.*, **160**, 103455. https://doi.org/10.1016/j.ijengsci.2021.103455.

Yang, F.A.C.M., Chong, A.C.M., Lam, D.C.C. and Tong, P. (2002), "Couple stress based strain gradient theory for elasticity", *Int. J. Solid Struct.*, **39**(10), 2731-2743. https://doi.org/10.1016/S0020-7683(02)00152-X.

Zeighampour, H. and Beni, Y.T. (2014), "Cylindrical thin-shell model based on modified strain gradient theory", *Int. J. Eng. Sci.*, **78**, 27-47. https://doi.org/10.1016/j.ijengsci.2014.01.004.

Zenggang, X., Zhiwen, T., Xiaowen, C., Xue-min, Z., Kaibin, Z. and Conghuan, Y. (2019), "Research on image retrieval algorithm based on combination of color and shape features", *J. Signal Proc. Syst.*, **93**(2), 139-146. https://doi.org/10.1007/s11265-019-01508-y.

Zhang, X., Wang, Y., Wang, C., Su, C. Y., Li, Z. and Chen, X. (2018), "Adaptive estimated inverse output-feedback quantized control for piezoelectric positioning stage", *IEEE T. Cybernet.*, **49**(6), 2106-2118. https://doi.org/10.1109/TCYB.2018.2826519.

Zhang, J., Wang, M., Tang, Y., Ding, Q., Wang, C., Huang, X. and Yan, F. (2021a), "Angular velocity measurement with improved scale factor based on a wideband-tunable optoelectronic oscillator", *IEEE T. Instrum. Meas.*, **70**, 1-9. https://doi.org/10.1109/TIM.2021.3067183.

Zhang, T., Wu, X., Shaheen, S.M., Rinklebe, J., Bolan, N.S., Ali, E.F. and Tsang, D.C. (2021b), "Effects of microorganism-mediated inoculants on humification processes and phosphorus dynamics during the aerobic composting of swine manure", *J. Hazard. Mater.*, **416**, 125738. https://doi.org/10.1016/j.jhazmat.2021.125738.

Zhang, L., Zheng, H., Wan, T., Shi, D., Lyu, L. and Cai, G. (2021c), "An integrated control algorithm of power distribution for islanded microgrid based on improved virtual synchronous generator", *IET Renew. Power Gener.*, **15**(12), 2674-2685. https://doi.org/10.1049/rpg2.12191.

Zhao, N., Deng, L., Luo, D. and Zhang, P. (2020), "One-step fabrication of biomass-derived hierarchically porous carbon/MnO nanosheets composites for symmetric hybrid supercapacitor", *Appl. Surf. Sci.*, **526**, 146696. https://doi.org/10.1016/j.apsusc.2020.146696

CC